Distribution of Chemical Pollutants in a Room Based on CFD Simulation Coupled with Emission/Sorption Analysis

Shuzo Murakami, Dr.Eng.
Member ASHRAE

Shinsuke Kato, Dr.Eng.
Member ASHRAE

Kazuhide Ito, Dr.Eng.

Akira Yamamoto

Yasushi Kondo, Dr.Eng.

Jun-ichi Fujimura

ABSTRACT

This paper presents physical models used in numerically analyzing the transportation of volatile organic compounds (VOCs) from building materials in a room. The models are based on fundamental physicochemical diffusion and adsorption/desorption (hereafter sorption) principles, both in the building materials and in room air. The performance of the proposed physical models is evaluated quantitatively in a test room using a technique that incorporates computational fluid dynamics (CFD). Two building materials are used in this study. One is a VOC-emission material whose emission rate is mainly controlled by the internal diffusion of the material. The other is an adsorbent material that has no VOC source, but it affects the room air concentration of VOCs through its sorption process. The emission material, made of SBR (polypropylene styrene-butadiene rubber), is situated on the floor. The adsorbent material, made of a charcoal-based activated carbon, is spread over the walls. The results of the numerical analysis show that the physical models and their numerical simulations effectively explain how VOCs are transported in a room.

INTRODUCTION

A method for predicting the distribution of chemical pollutants emitted in a room was investigated. Indoor air quality is greatly affected by the emission and sorption of chemical compounds from building materials (Haghighat and de Bellis 1998; Meininghaus et al. 1998; Chang et al. 1992; Christianson et al. 1993; Bluyssen et al. 1995). In this study, physical models of emission and sorption of volatile organic compounds (VOCs) are proposed. The models are based on the fundamental physicochemical principles of diffusion and sorption of VOCs in both building materials and room air.

To demonstrate the validity of the models, concentration distributions of VOCs in a room are analyzed quantitatively using a computational fluid dynamics (CFD) technique. Here the emission material, made of SBR, is situated on the floor [note 1]. The emission rate of VOCs from SBR is mainly controlled by internal diffusion in the material (Yang et al. 1998). In this study, a charcoal-based activated carbon is used as the adsorbent material, which has no source of VOCs and affects room air concentration only through its sorption process. It is spread over the walls.

It is assumed that the composition ratio of VOCs does not change; a virtual VOC species representing the total property of VOCs emitted into the air is used in this study. The virtual VOC is defined in this paper as a representative VOC (or simply VOCs).

Many factors, including emission, adsorption/desorption, air change rate, and chemical reactions within the source material and the room air, affect the concentration of chemical pollutants within a room (Wolkoff and Nielsen 1996; Murakami et al. 1999). The goal of this study is to predict the concentration of chemical pollutants in the air inhaled by the occupants of the room.

PHYSICAL MODELS OF VOC TRANSFER

Transportation in Room Air

VOCs emitted from building materials are transported by the convection of the room air and dispersed by molecular diffusion (λ_a/ρ_{air} [m²/s]) and turbulent diffusion (v_t/σ [m²/s]) (cf. Figure 1). The vapor phase concentration C (kg_{VOCs}/kg_{air})

Shuzo Murakami and **Shinsuke Kato** are professors at the Institute of Industrial Science (IIS), University of Tokyo. **Kazuhide Ito** is a research associate at the Tokyo Institute of Polytechnics. **Akira Yamamoto** is a graduate student at IIS. **Yasushi Kondo** is an associate professor and **Jun-ichi Fujimura** is a graduate student at the Musashi Institute of Technology, Japan.
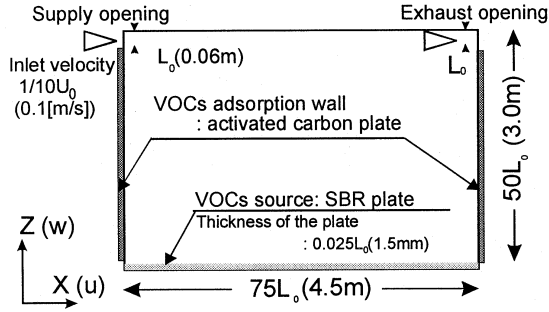
Figure 1 *Room model.*

of VOCs in the room air can be described by the mass conservation equation as given in Equation 1:

$$\rho_{air}\frac{\partial C}{\partial t} + \rho_{air}\frac{\partial(u_j C)}{\partial x_j} = \frac{\partial}{\partial x_j}\left(\left(\lambda_a + \frac{\rho_{air}v_t}{\sigma}\right)\frac{\partial C}{\partial x_j}\right) \qquad (1)$$

Here, ρ_{air} (kg/m³) is the air density, λ_a (kg/[ms kg/kg]) is the molecular mass conductivity, v_t (m²/s) is the turbulence eddy viscosity, and σ is the turbulent Plandtl number (= 1.0). Velocity u_j (m/s) and v_t are given by solving for the flow field with a low Reynolds number type k-ε turbulence model. Thus, Equation 1 is closed.

Diffusive and Adsorptive Transportation in Materials

The transportation of VOCs in building materials (internal diffusion or permeation) is possible because of the fine pores found in the materials. However, the diffusive transport of VOCs within such porous materials is very complex. Molecular and Knudsen diffusions in the vapor phase occur through the pores in the materials due to the concentration gradient. On the surface of the pores, vapor-phase VOCs are adsorbed and desorbed as shown in Figure 2. We may assume that the VOC diffusion within the nonporous part of the material is so small that the diffusion here may be disregarded when compared with that which diffuses through the pores. VOC transportation through the pores and on the surface of the pores can be described by the conservation equations (2 and 3), respectively. Equation 2 is a diffusion equation through the pores with source and sink terms (sorptive effect).

$$k\rho_{air}\frac{\partial C}{\partial t} = \frac{\partial}{\partial x_j}\left(\lambda_C\frac{\partial C}{\partial x_j}\right) - adv \qquad (2)$$

$$\rho_{sol}\frac{\partial C_{ad}}{\partial t} = adv \qquad (3)$$

Here C (kg/kg) is the vapor phase concentration in the pores, C_{ad} (kg/kg) is the solid (adsorbed) phase concentration on the surface of a pore, ρ_{sol} (kg/m³) is the net density of the adsorbent material, λ_C (kg/[ms kg/kg]) is the mass conduc-
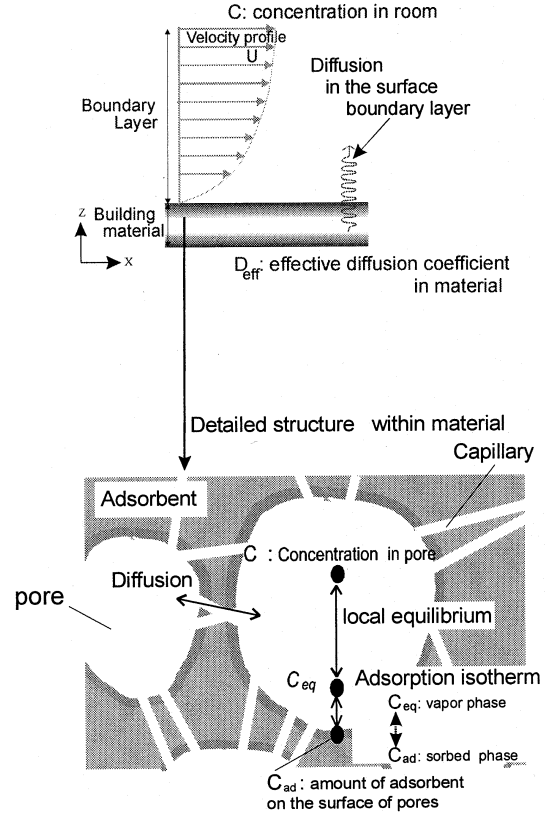

Figure 2 *Modeling of VOC diffusion and adsorption in the material.*

tivity of VOCs in air within the pores, and k (m³/m³) is the porosity of the material [note 2].

Substituting Equation 3 into Equation 2, the diffusion and adsorption equation for the material is obtained and given as Equation 4.

$$k\rho_{air}\frac{\partial C}{\partial t} = \frac{\partial}{\partial x_j}\left(\lambda_C\frac{\partial C}{\partial x_j}\right) - \rho_{sol}\frac{\partial C_{ad}}{\partial t} \qquad (4)$$

Equation 4 is not closed since it includes two unknowns, C and C_{ad}.

Generalized Adsorption Isotherm

In order to close Equation 4, a so-called adsorption isotherm is introduced. For closed systems under steady state, the rate of adsorption is equal to the rate of desorption, thus achieving equilibrium. Since this phenomenon of sorptive dynamics occurs much more rapidly than that of molecular diffusion in a gas, in a small CV (control volume) under the isothermal conditions at constant pressure, an equilibrium relation between the concentration in a gas and that on an adsorbent surface can be realized. The relation is expressed by the so-called general adsorption isotherm (Equation 5).

$$C_{ad} = f(C_{eq}, T) \qquad (5)$$

Here the function f is unique for a combination of adsorbed compounds and adsorbents. T (K) is the absolute temperature.

The time differential of C_{ad} is expressed as Equation 6.

$$\frac{\partial C_{ad}}{\partial t} = \frac{\partial f}{\partial C_{eq}}\frac{\partial C_{eq}}{\partial t} + \frac{\partial f}{\partial T}\frac{\partial T}{\partial t} \tag{6}$$

Since C in the pores becomes identical to C_{eq} as stated in Note 2, C can be substituted for C_{eq} in the small CV, including the adsorbent surface.

Simple Transportation Model Governed by Effective Diffusion

Equation 4, for diffusion and adsorption in porous materials, is reexpressed as Equation 7 using the relation of the adsorption isotherm (Equation 6).

$$\left(k\rho_{air} + \rho_{sol}\frac{\partial f}{\partial C}\right)\frac{\partial C}{\partial t} = \frac{\partial}{\partial x_j}\left(\lambda_C\frac{\partial C}{\partial x_j}\right) - \rho_{sol}\frac{\partial f}{\partial T}\frac{\partial T}{\partial t} \tag{7}$$

In Equation 7, the assumption of local equilibrium in a pore ($C_{eq} = C$) is applied. When conditions are isothermal (temperature held constant), $\partial T/\partial t$ can be omitted and Equation 7 thus becomes

$$\left(k\rho_{air} + \rho_{sol}\frac{\partial f}{\partial C}\right)\frac{\partial C}{\partial t} = \frac{\partial}{\partial x_j}\left(\lambda_C\frac{\partial C}{\partial x_j}\right). \tag{8}$$

Equation 8 can be rewritten for simple diffusion as Equations 9 and 10.

$$\rho_{air}\frac{\partial C}{\partial t} = \frac{\partial}{\partial x_j}\left(\rho_{air}D_C\frac{\partial C}{\partial x_j}\right) \tag{9}$$

$$D_C = \lambda_C \bigg/ \left(k\rho_{air} + \rho_{sol}\frac{\partial f}{\partial C}\right) \tag{10}$$

where D_C (m²/s) is the effective diffusion coefficient of VOCs in the material concerned [Note 1]. C (kg/kg) is the vapor phase concentration in the pores. The equations are closed when isotherm models such as Equations 15 and 17 are introduced as described later. Vapor phase concentration C is related to the solid (adsorbed) phase concentration C_{ad} in the substance (adsorbent) with the adsorption isotherm of Equation 5 through the assumption of $C = C_{eq}$. In this context, the vapor phase concentration C represents the total VOC concentration in the material. In this study, the vapor phase concentration C is used as the equivalent vapor phase concentration to express the concentration in the material instead of the solid phase concentration C_{ad} (Sparks et al. 1996; Yang et al. 1998; Murakami et al. 1998) [note 1].

Boundary Conditions at the Air-Material Interface

Since the transportation of C in the material and in the room air is solved simultaneously, a boundary condition should be set at the air-material interface. The VOC emission

rate at the air-material interface should be the same as the transportation rate of internal diffusion from the inside. This condition is expressed as the conservation law at the surface of the material, as shown in Equation 11.

$$-\rho_{air}D_C\frac{\partial C}{\partial x}\bigg|_{B+} = -\lambda_a\frac{\partial C}{\partial x}\bigg|_{B-} \tag{11}$$

Here, $B+$ is the air-material surface in the material-side region, and $B-$ is that in the air-side region. Equation 11 is used as the boundary condition at the air-material interface when the transportation in the material and the room air is solved simultaneously.

SIMPLE TRANSPORTATION MODEL ON SORPTIVE SURFACES

In general, the diffusion and adsorption process in a material can be described using the effective diffusion coefficient D_C, which implicitly includes the effect of sorption [Note 2]. If the material has no VOC source and it contributes to the room air concentration only through its sorptive process, modeling the sorption process is simpler than described above. For simple modeling, it is assumed that adsorption occurs only on the surface (Figure 3). VOC transfer near building materials is also governed by Equations 2 and 3, as well as the phenomenon within the material. Here, two CVs (dV [m³]) are set at the interface to simplify modeling of the transportation on adsorbent material as shown in Figure 3. The two CVs have a common surface element dS (m²). The layer dh (m) normal to the surface element dS is very thin. The surface element dS is sandwiched by the CVs, i.e., by the CV in the material and in the air. Here, dh is assumed to be so small that the sorption process attains equilibrium immediately in the CV, and, consequently, the time differentiation of the vapor-phase concentration can be omitted. When volume integration is performed for Equations 2 and 3 in each CV, omitting the time differential term of the vapor-phase concentration in air, the following equations are given.
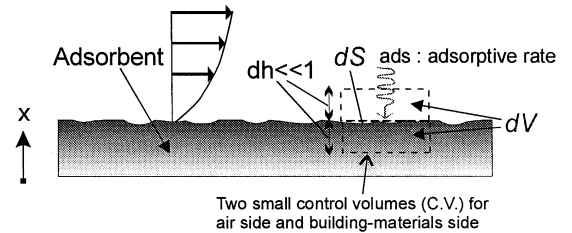
dV : volume of the CV
dS : surface element of the CV
dh : thin thickness of the CV

Figure 3 *Modeling of adsorption and desorption of VOCs on the surface of sorptive material.*

CV in the air:

$$0 = \lambda_a \frac{\partial C}{\partial x}\bigg|_{B-} dS - adv \cdot dV \qquad (12)$$

CV in the material:

$$\rho_{sol} \frac{\partial C_{ad}}{\partial t} dV = adv \cdot dV \qquad (13)$$

With Equations 12 and 13, the VOC adsorption rate on the surface of the material is related to the molecular diffusion of VOCs close to the surface of the adsorbent, as shown in Equation 14.

$$-\lambda_a \frac{\partial C}{\partial x}\bigg|_{B-} = -adv \cdot \frac{dV}{dS} = -ads = -\left(\rho_{sol}\frac{\partial C_{ad}}{\partial t}\right)\frac{dV}{dS} = -\rho'_{sol}\frac{\partial C_{ad}}{\partial t}$$

$$(14)$$

Here, ads (kg/m^2·s) is the adsorption/desorption rate (positive/negative ads corresponds to the adsorption/desorption rates, respectively), and ρ'_{sol} ($= \rho_{sol}\, dV/dS$, kg/m^2) is the plane density of a sorptive material.

Typical Isotherm Models

Two types of adsorption isotherm are used in this study: the Henry model and the Langmuir model.

The Henry Model. For adsorption under low concentration of VOCs in air, the Henry model (usually called "the linear model") is utilized.

$$C_{ad} = k_h \cdot C_{eq} \qquad (15)$$

Here, k_h (-) is Henry's coefficient. The adsorption term in Equation 14 is rewritten as Equation 16.

$$\lambda_a \frac{\partial C}{\partial x}\bigg|_{B-} = ads = \rho'_{sol}\frac{\partial C_{ad}}{\partial t} = \rho'_{sol}\frac{\partial k_h \cdot C_{eq}}{\partial t} = \rho'_{sol}k_h\frac{\partial C|_{B-}}{\partial t}$$

$$(16)$$

Equation 16 is used as the boundary condition for the sorptive surface when solving Equation 1. In the numerical simulation, the VOC concentration in the air-side CV adjacent to the material is assumed to be the same as the concentration in the equilibrium state, i.e., $C|_{B-} = C_{eq}$.

The Langmuir Model. When the VOC concentration in room air becomes high, the concentration of adsorbed VOCs, C_{ad}, on the adsorbent is saturated at a certain level of room air concentration. In this case, the Henry model overestimates the amount of adsorbed VOCs. The Langmuir model is based on a model of monolayer adsorption, which takes into account the concept of saturating concentration, C_{ad0}. The Langmuir model, which can be applied to a higher VOC concentration field, is thus more sophisticated than the Henry model. It is expressed by Equation 17 [note 3].

$$C_{ad} = \frac{C_{ad0}k_l C_{eq}}{1 + k_l C_{eq}} \qquad (17)$$

Here, k_l (1/(kg/kg)) is Langmuir's coefficient and C_{ad0} (kg/kg) is the concentration of the saturated adsorption by monolayer adsorption. The adsorption term in Equation 14 is rewritten as Equation 18 in the same manner as Equation 16.

$$\lambda_a \frac{\partial C}{\partial x}\bigg|_{B-} = ads = \rho'_{sol}\frac{\partial C_{ad}}{\partial t} = \frac{\rho'_{sol}C_{ad0}k_l}{(1 + k_l C|_{B-})^2} \cdot \frac{\partial C|_{B-}}{\partial t} \qquad (18)$$

Equation 18 is used as the boundary condition for the sorptive surface when solving Equation 1.

Sets of Equations for Coupled Simulation

Set 1: equations for emission surface simulation

For coupled simulation of VOC transportation between the room air and the material with VOC emission, Equations 1, 9, 10, 11, and 16 or 18 are solved simultaneously.

*Set 2: equations for adsorption/desorption surface simulation*

For coupled simulation of VOC transportation between the room air and the sorptive material, Equations 1 and 14 or 16 or 18 are solved simultaneously. Set 2 is much simpler than Set 1 because of the simplified modeling of the sorption phenomenon. Set 2 does not calculate the internal diffusion within the material. Consequently, Set 2 has the advantage of a much lighter CPU load. However, the modeling of the sorptive phenomenon itself in Set 2 becomes clearer than that in Set 1. These two sets of equations are applied simultaneously in the case study described later (cf. Figure 2).

ROOM MODEL AND BUILDING MATERIALS USED

The room model (two-dimensional) used for simulation is shown in Figure 1. It was used to analyze diffusion in the room air and also emission/sorption processes of the VOCs of the building materials. The room model has dimensions of $(x) \times (z) = 75\, L_0 \times 50\, L_0$ ($= 4.5$ m $\times 3.0$ m; $L_0 = 0.06$ m $=$ width of supply inlet). A polypropylene styrene-butadiene rubber (SBR) plate (0.025 L_0 thick: 1.5×10^{-3} m) was selected as a VOC source and attached to the floor [note 1]. The emission rate from the material is strongly related to both the initial concentration distribution C_0 and the effective diffusion coefficient D_C within the SBR.

In this study, the initial VOC concentration distribution in the SBR is assumed to be uniform, $C_0 = 0.16$ kg/kg. It is assumed that a new carpet has been laid. The effective diffusion coefficient D_C is assumed to be 1.1×10^{-14} m^2/s at 23°C, following Yang et al. (1998). The diffusion of VOCs at the side face and bottom are assumed to be cut off. As an adsorptive surface, a charcoal-based activated carbon was spread over the walls. The adsorption capacity depends on the surface area of the adsorbent. The activated carbon has a wide surface area of more than 10^6 m^2/kg.

In this study, the plane density ρ'_{sol} is set to 1×10^{-6} kg/m^2, i.e., the surface area of the adsorbent is the same as that of the building materials. This value is quite small from a practical
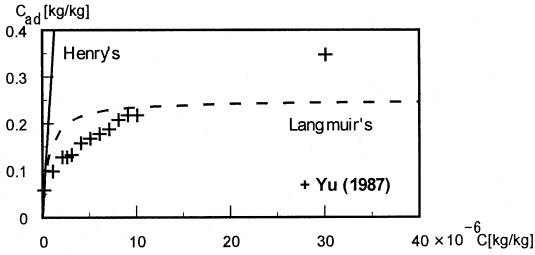
(a) C_{eq} vs. C_{ad} in high concentrations of C_{eq}
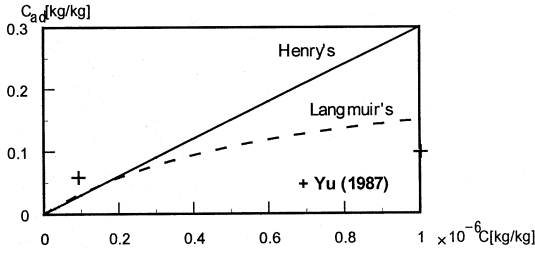
(b) C_{eq} vs. C_{ad} in low concentrations of C_{eq}

C_{eq} : vapor concentration at equilibrium state
C_{ad} : amount of adsorption

Figure 4 *Representative isotherm model and experimental data.*

viewpoint. The parameters in the sorptive isotherm are estimated following the experiment in which toluene is adsorbed on a charcoal-based activated carbon at 25°C. Here, as shown in Figure 4, we assume Henry's coefficient k_h is 3.0×10^5 and Langmuir's coefficient k_l is 1.5×10^6 (1/[kg/kg]). The concentration of saturating adsorption C_{ad0} is 0.25 kg/kg (Yu 1987; Axley 1995).

NUMERICAL METHODS AND BOUNDARY CONDITIONS

Table 1 shows the numerical conditions. The flow fields were analyzed with a low Reynolds number k-ε model (Murakami et al. 1996) [Note 4] with an inflow velocity of 0.1 U_0 (= 0.1 m/s; air change rate = 1.6 h^{-1}). A centered differential scheme is used for the convection term in air. Using the results of the flow field simulations, the behavior of VOC transportation was analyzed. At floor level, where both emission and internal diffusion are observed, time-dependent Equations 1 and 10 were solved by combining them with Equation 12. At the walls where adsorption is observed, Equation 1 was solved by coupling it with Equation 14 using the models of adsorption isotherm Equation 16 or 18. These two parts, i.e., the emission and internal diffusion part (floor) and the adsorption part (side walls), were solved simultaneously. Table 2 shows the analysis of the cases. Nine cases were examined in total, with different values of the coefficients k_h, k_l, and C_{ad0}. The time-history of the room air concentration was obtained over a duration of

TABLE 1
Numerical Conditions

Number of grid points (2D)	
Air region: $\qquad$ $68(x) \times 64$ $(z) = 4.5$ mm (W) $\times$ 3.0 m (H) Material region dominated by internal diffusion: $\qquad$ $68(x) \times 41$ $(z) = 4.5$ mm (W) $\times$ 1.5×10^{-3} m (H) Width of mesh adjacent to the surface: $\qquad$ 0.6×10^{-9} mm Region of adsorptive surface for side walls: $\qquad$ $55(z) = 2.94$ m (H)	
Reynolds number	$U_0 L_0/v = 4.2\times10^3$
Molecular diffusion coefficient of VOCs in air	$\lambda_a / \rho_{air} = 5.9\times10^{-6}$ m^2/s (23ºC)
Effective diffusion coefficient of VOCs in the material (Yang et al. 1998)	$D_C = 1.1\times10^{-14}$ m^2/s (23ºC)
Inflow velocity	0.1 $U_0 = 0.1$ m/s

TABLE 2
Cases Analyzed

| Isotherm model/Case no.	Applied parameters	
Case 1	Carpet only	
Henry model	Henry's coefficient: k_h [-]	
Case 2-1	3.0×10^4	
Case 2-2	3.0×10^5	
Case 2-3	3.0×10^6	
Langmuir model	k_l^*	$C_{ad0}^\dagger$
Case 3-1	1.5×10^6	
Case 3-2	1.5×10^5	0.25
Case 3-3	1.5×10^7	
Case 3-4	1.5×10^6	0.025
Case 3-5		2.5

* Langmuir's coefficient: k_l [1/(kg/kg)]
† The amount of saturating adsorption : C_{ad0} [kg/kg]

7.2×10^6 T_0 (five days, T_0, a representative time scale defined by L_0/U_0).

RESULTS AND DISCUSSION

For the flow field of the model room (cf. Figure 5), we conducted a precise modeling experiment using identical Reynolds numbers as simulations. Details of the modeling experiment are reported in Murakami et al. (1996). The velocity distribution given from the prediction with the low Reynolds number k-ε model and the results obtained in the model experiment are in very close agreement (Suzuki et al. 1996; Murakami et al. 1998).
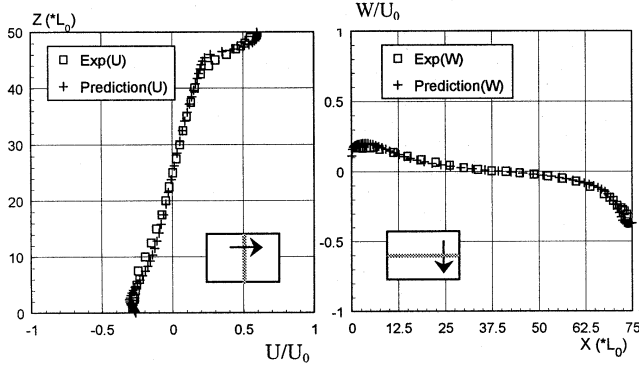
(1) Vertical profile of U/U$_0$ (2) Horizontal profile of W/ U$_0$

(x=37.5L$_0$ line)   W (z=25L$_0$ line)

Figure 5 *Flow field comparison between prediction and experiment.*

VOC Concentration in Room Air

As shown in Figure 6a, the maximum value of room-averaged VOC concentration C_{max} reaches 0.165 kg/kg in case 1 just after the start of the time-dependent numerical simulation. Such a pattern in the time-history can be regarded as similar to the VOC emissions found in a room furnished with newly produced materials. Here, the C_0 distribution in SBR is assumed to be uniform as described before. The computation begins with an initial condition of zero concentration in the room. The room-averaged VOC concentration declines gradually over a duration of $7.2 \times 10^6 \, T_0$ (five days) after reaching a peak. The time histories of room-averaged concentration in cases 2-1 and 2-2 are almost the same as in case 1. In this analysis, the sorption effect is observed only within a period of six hours, around the time when the VOCs reach their peak concentrations. After 24 hours, the time-dependent term of VOC concentration in room air $\partial C / \partial t$ becomes so small that the effect of sorption on the room air becomes negligible. However, we noted that in this study the smallest amount of adsorbent is spread on the walls. In the Henry model, the increase of k_h has the same effect on the increase of ρ'_{sol} (see Equation 16), and the adsorbed amount is proportional to the product of ρ'_{sol} and k_h. In cases 2 and 3 of Figure 6a, the peak value of the room-averaged concentration falls because of the higher value of k_h. We can thus conclude that a larger value of ρ'_{sol} also has the effect of decreasing the peak values.

As shown in Figure 6b, the simulation with the Langmuir model also shows that the effect of the adsorbent is almost negligible when the quantity of the adsorbent is very small, as is the case in this study. Comparisons between case 1, case 2-2, and case 3-1 show the effect of using different adsorption models on the room-averaged concentration. Since the quantity of the sorptive material is very small, only minor differences are seen in the results of the three cases. However, the
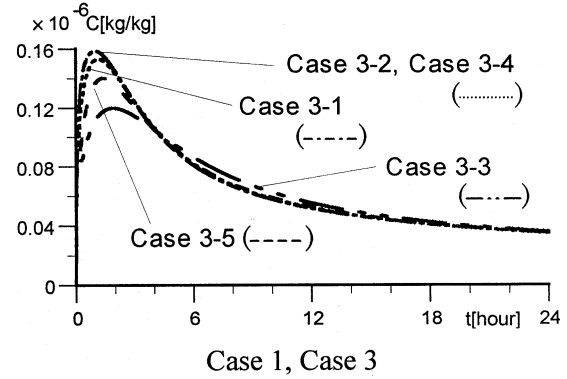

Case 1, Case 3

Figure 6 *Time history of room-averaged concentrations.*

peak concentration in case 2-2 is the lowest and that of case 1 is the highest.

We can see that the sorption effect definitely reduces the peak concentration and also that the Henry model has a tendency to overestimate the effect. The Henry model has the disadvantage of overestimating adsorption in high concentration regions of room air compared with the Langmuir model, as shown in Figure 6b.

The time-history of the room-averaged concentrations are compared in Figure 6c using different parameters in the Langmuir model. When Langmuir's coefficient, k_l, or the concentration of saturated adsorption, C_{ad0}, is high, the maximum room-averaged concentration decreases and the concentration dissipates slowly.

The room-averaged concentration after 120 hours falls to 1.57×10^{-8} kg/kg, or nearly one-tenth of the peak value. Under these conditions, the concentration field nearly reaches a steady state. The spatial distribution of VOC concentration in the room 24 hours after the start of the simulation is shown in Figure 7. The local concentration is higher near the floor. The maximum value of concentration is observed near the floor in the left-hand corner of the room. This value is 3.89×10^{-8} kg/kg, which is 2.4 times higher than the mean concentration. This higher concentration means that children or people sleeping on the floor are likely to be exposed to higher VOC concentrations.

Amount of Adsorption on the Adsorbent

The room air concentration of VOCs near the left-hand wall is four times higher than that near the right-hand wall, as shown in Figure 7. This difference is caused by the clockwise circulation of the air and the placement of the contaminant source on the floor. The amount of adsorbate at the left-hand wall, therefore, is four times larger than that at the right-hand wall. The time histories of the mean amount of adsorbate at the left-hand wall are shown in Figure 8. The larger value of Henry's coefficient leads to a higher amount of adsorbate, as is shown in Figure 8a. As with the Henry model, the larger
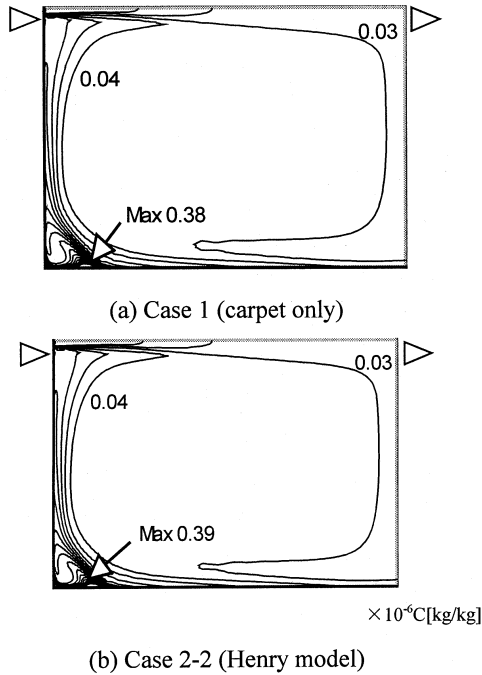
(a) Case 1 (carpet only)

$\times 10^{-6} C$[kg/kg]

(b) Case 2-2 (Henry model)

Figure 7 *Concentration distribution of VOCs (24 hours after the start of analysis).*

(a) Case 2-1, Case 2-2, Case 2-3

(b) Case 3-1 ~ Case 3-5

Figure 8 *Time history of the amount of VOCs adsorbed by sorptive material.*

value of Langmuir's coefficient, k_l, or the higher concentration of saturated adsorption, C_{ad0}, leads to a higher adsorption.

CONCLUDING REMARKS

1. The physical model of VOC emission, where the emission rate is controlled by internal diffusion, was deduced and applied to the SBR plate in a room. The adsorption effect of building materials was modeled simply and included in the predictive model of the VOC concentration in room air. The model was applied to the adsorption by the charcoal-based activated carbon that was spread thinly on the walls.

2. The room-averaged VOC concentration fell gradually throughout the duration of the analysis (7.2×10^6 T_0, five days). The adsorption effect on the room air concentration becomes clear when the room air concentration changes rapidly.

3. The amount of adsorbate on the walls increases in proportion to the rise in Henry's coefficient. The predicted results of Henry's model tend to overestimate the amount of adsorbate when the room air concentration rises. The Henry model addresses this problem. The higher value of the concentration of saturating adsorption, C_{ad0}, and the addition of Langmuir's coefficient, k_l, lead to a larger quantity adsorbed and a decrease in the room-averaged concentration of VOCs.

Note 1

VOC emission materials have the potential of adsorbing VOCs in room air. However the vapor-phase concentration of the emitting surface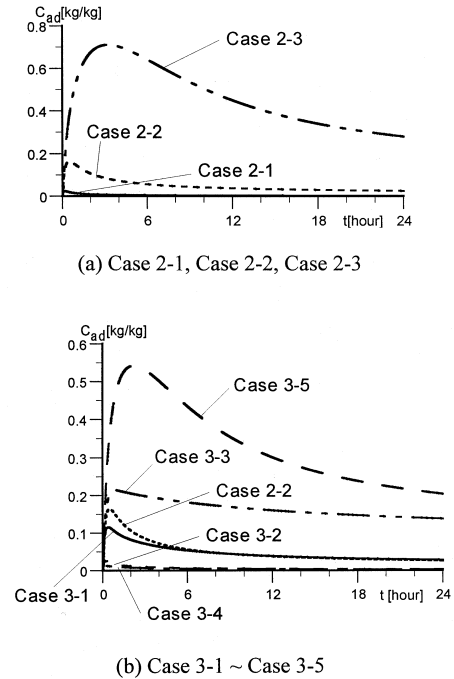 of the material is usually much higher than the VOC concentration of the room air near the surface. Thus, emission materials apparently have no practical effect in adsorbing VOCs from room air in practice. Equation 9, which uses the effective diffusivity Dc, includes the effect of adsorption implicitly, as shown in the definition of Dc in Equation 10. It possesses a potential sorptive effect, i.e., the term of $\rho_{sol}\partial f/\partial C$ in the denominator of Equation 10. In Equation 9, the left-hand term indicates the decrease/increase of VOC amount per unit time, i.e., it shows a dynamic change in the storage quantity of VOCs in the materials. Most of this dynamic storage effect is attributable to the sorptive effect described by the effective diffusivity Dc in Equation 10.

Note 2

The mass transportation within the pores to the surface of the adsorbent is adv (kg/m^3·s), which is defined as follows:

$$adv = -\alpha S(C_{eq} - C) \qquad (a)$$

Here, C_{eq} (kg/kg) is the vapor phase concentration in equilibrium with the solid phase concentration, C_{ad}, on the surface of the material; α (kg/[m^2·s kg/kg]) is the sorptive rate between the pores and the surface; and S (m^2/m^3) is the surface area of the pores per unit volume. When a closed system is assumed within a pore under constant conditions, the vapor phase concentration C in the pores moves toward the equilibrium concentration C_{eq}, and thus mass transportation adv becomes zero in a closed system.

Note 3

Langmuir proposed a model for adsorption that assumed there are active points on the surface of the adsorbent and that

adsorbates can be adsorbed on these points up to a limit. When the ratio of the adsorbed area is described by θ (-), the desorption rate of adsorbate r (kg/m$^2\cdot$s) is expressed as Equation b:

$$r = k_d\theta \tag{b}$$

Here, k_d (kg/m$^2\cdot$s) is the desorption coefficient. Thus, the adsorption rate of adsorbate r' (kg/m$^2\cdot$s) is expressed as Equation c:

$$r' = k_aC(1 - \theta) \tag{c}$$

Here, k_a (kg/[m$^2\cdot$s kg/kg]) is the adsorption coefficient. In a state of equilibrium, r becomes equal to r' and the concentration C converges with C_{eq}. Consequently, Equation d is given.

$$\theta = \frac{(k_a/k_d)C_{eq}}{1 + (k_a/k_d)C_{eq}} \tag{d}$$

θ can be described simply as Equation e, using a solid phase concentration C_{ad} (kg/kg) and the saturating concentration C_{ad0} (kg/kg).

$$\theta = C_{ad} / C_{ad0} \tag{e}$$

Then,

$$C_{ad} = \frac{C_{ad0}k_lC_{eq}}{1 + k_lC_{eq}} \tag{f}$$

Here, k_l (1/[kg/kg]), defined by k_a/k_d, is the Langmuir coefficient.

Note 4

In this study, flow fields were analyzed with a low Reynolds number k-ε model (MKC model, Murakami et al. 1996). The governing equation of the MKC model shows the following. An overbar ($^{-}$) denotes the ensemble mean value. This model has been used successfully to predict both a flow within the laminar region near the wall and a far wall region.

$$\frac{\partial \overline{U}_i}{\partial t} + \overline{U}_j \cdot \frac{\partial \overline{U}_i}{\partial x_j} = -\frac{1}{\rho}\cdot\frac{\partial \overline{P}}{\partial x_i} + v\frac{\partial}{\partial x_j}\left(\frac{\partial \overline{U}_i}{\partial x_j} + \frac{\partial \overline{U}_j}{\partial x_i}\right) - \frac{\partial}{\partial x_j}\overline{u_i'u_j'} \tag{g}$$

$$-\overline{u_i'u_j'} = v\left(\frac{\partial \overline{U}_i}{\partial x_j} + \frac{\partial \overline{U}_j}{\partial x_i}\right) - \frac{2}{3}k\delta_{ij} \tag{h}$$

$$v_t = c_\mu \cdot f_\mu \cdot k^2/\varepsilon \tag{i}$$

$$\frac{\partial k}{\partial t} + \overline{U}_j\frac{\partial k}{\partial x_j} = D_k + P_k - (\bar{\varepsilon} + D) \tag{j}$$

$$\frac{\partial \bar{\varepsilon}}{\partial t} + \overline{U}_j\frac{\partial \bar{\varepsilon}}{\partial x_j} = D_\varepsilon + \frac{\bar{\varepsilon}}{k}\cdot(C_{\varepsilon1}\cdot f_1\cdot P_k - C_{\varepsilon2}\cdot f_2\cdot \bar{\varepsilon}) + E \tag{k}$$

$$P_k = \overline{u_i'u_j'}\cdot\frac{\partial \overline{U}_j}{\partial x_i} \tag{l}$$

$$D_k = \frac{\partial}{\partial x_j}\cdot\left(\left(v + \frac{v_t}{\sigma_k}\right)\frac{\partial k}{\partial x_j}\right) \tag{m}$$

$$D_\varepsilon = \frac{\partial}{\partial x_j}\cdot\left(\left(v + \frac{v_t}{\sigma_\varepsilon}\right)\frac{\partial \bar{\varepsilon}}{\partial x_j}\right) \tag{n}$$

$$\bar{\varepsilon} = \varepsilon - 2v\left(\frac{\partial \sqrt{k}}{\partial x_k}\right)^2 \tag{o}$$

$$f_\mu = \left\{1 - \exp\left(\frac{y^*}{14}\right)\right\}^2\left[1 - \exp\left(-\frac{R_t^{3/4}}{2.4}\right)\right]\cdot\left[1 + \frac{1.5}{R_t^{5/4}}\right] \tag{p}$$

$$f_1 = 1.0 \tag{q}$$

$$f_2 = \left\{1 - \exp\left(-\frac{y^*}{3.1}\right)\right\}^2\left[1 - 0.3\cdot\exp\left\{-\left(\frac{R_t}{6.5}\right)^2\right\}\right] \tag{r}$$

$$\bar{\varepsilon} = \varepsilon = 2v\left(\frac{\partial \sqrt{k}}{\partial y}\right)^2 \tag{s}$$

$$\frac{l}{\eta} = R_t^{3/4} \tag{t}$$

$$R_t = \frac{k^2}{v\varepsilon} \text{ (turbulent Reynolds number)} \tag{u}$$

$$l = \frac{k^{3/2}}{\varepsilon} \text{ (turbulent length scale)} \tag{v}$$

$$y^* = \frac{u_\varepsilon y}{v} = \frac{y}{\eta}$$
(nondimensional length from wall surface) $\tag{w}$

$$\eta = \frac{v^{3/4}}{\varepsilon^{1/4}} \text{ (Kolmogorov length scale)} \tag{x}$$

$$u_\varepsilon = (v\varepsilon)^{1/4} \text{ (Kolmogorov velocity scale)} \tag{y}$$

$$C_\mu = 0.09, \sigma_k = 1.4, C_{\varepsilon1} = 1.5, C_{\varepsilon2} = 1.9, \sigma_\varepsilon = 1.4, D = E = 0$$

REFERENCES

Axley, J.W. 1995. New mass transport elements and compounds for the NIST IAQ model. *NIST GCR*, pp. 95-676. Gaithersburg, Md.: National Institute of Standards and Technology.

Bluyssen, P.M., et al. 1995. European database of indoor air pollution sources: The effect of temperature on the chemical and sensory emissions of indoor materials. TNO-Report 95-BBI-R0826.

Chang, J.C.S. et al. 1992. Characterization of organic emissions from a wood finishing product—wood stain. *Indoor Air* 2: 146-153.

Christianson, J., J.W. Yu, et al. 1993. Emission of VOCs from PVC-flooring models for predicting the time-dependent emission rate and resulting concentration in indoor air. *Proceedings of Indoor Air '93*, vol. 2, pp. 389-394.

Haghighat, F., and L. de Bellis. 1998. Material emission rates: Literature review and the impact of indoor air temperature and relative humidity. *Building and Environment* 33: 261- 277.

Meininghaus, R, H.N. Knudsen., and L. Gunnarsen. 1998. Diffusion and sorption of volatile organic compounds in indoor surface materials. *EPIC'98, Lyon, France, 19-21 November*, vol. 1, pp. 33-38.

Murakami, S., et al. 1996. New low Reynolds number *k*-ε model including damping effect due to buoyancy in a stratified flow field. *Int. J. Heat Mass Transfer* 39: 3483-3496.

Murakami, S., et al. 1999. Coupled analysis of emission, sorption and diffusion of chemical pollutants in a ventilated room by CFD. *Indoor Air '99, Edinburgh*.

S. Murakami, S. Kato, and K. Ito. 1998. Coupled analysis of VOCs emission and diffusion in a ventilated room by CFD. *EPIC'98, Lyon, France, 19- 21 November*, vol. 1, pp. 19-26.

Sparks, L.E., B.A. Tichenor, J. Chang, and Z. Guo. 1996. Gas-phase mass transfer model for predicting volatile organic compound (VOC) emission rates from indoor pollutant sources. *Indoor Air* 6: 31-40.

Suzuki, N., et al. 1996. Study on evaluation of ventilation effectiveness of occupied space in a room (part 3). Precise model experiment of airflow in a room for analyzing PFR. *SHASE Transactions*, pp. 45-48 (in Japanese).

Wolkoff., P., and P. Nielsen. 1996. A new approach for indoor climate labeling of building materials—Emission testing, modeling, and comfort evaluation. *Atmospheric Environment* 30(15): 2679-2689.

Yang, X., Q. Chen, and P.M. Bluyssen. 1998. Prediction of short-term and long-term volatile organic compound emissions from SBR bitumen-backed carpet at different temperatures. *ASHRAE Transactions* 104(2): 1297-1308.

Yu, J.-W. 1987. Adsorption of trace organic contamination in air. Stockholm: Royal Institute of Technology.